Calcif Tissue Int (2008) 82:77–86
DOI 10.1007/s00223-007-9093-2

# The Effects of Bone Remodeling Inhibition by Alendronate on Three-Dimensional Microarchitecture of Subchondral Bone Tissues in Guinea Pig Primary Osteoarthrosis

**Ming Ding · Carl Christian Danielsen · Ivan Hvid**

Received: 6 June 2007 / Accepted: 6 November 2007 / Published online: 4 January 2008


**Abstract** We assessed whether increase of subchondral bone density enhances cartilage stress during impact loading, leading to progressive cartilage degeneration and accelerated osteoarthrosis (OA) progression. Sixty-six male guinea pigs were randomly divided into six groups. During a 9-week treatment period, four groups received twice-weekly subcutaneous injections of alendronate (ALN) in two doses: two groups received 10 μg/kg and two groups received 50 μg/kg. The two control groups received vehicle. After 9 weeks, one 10 μg/kg ALN group, one 50 μg/kg ALN group, and one control group were killed. The remaining three groups (17-week groups) were left for an additional 8 weeks, receiving the same treatment regimen before death. The left proximal tibiae were scanned by micro-computed tomography to quantify the microarchitecture of subchondral bone, followed by mechanical testing and determination of collagen and mineral. The control groups had typical OA-related cartilage degeneration at 9 and 17 weeks, whereas the 50 μg/kg ALN group had even worse degeneration in the medial condyle. It is unclear whether there is a direct or a secondary effect of ALN on the cartilage. The 9-week ALN group had significantly greater subchondral plate thickness. The 9- and 17-week groups had similar changes of cancellous bone microarchitecture, with greater volume fraction and connectivity and an extremely plate-like structure. The 9-week ALN group had greater bone mineral concentration, and the 17-week ALN group had reduced collagen concentration and greater mineral concentration. Treatment with ALN did not significantly change the mechanical properties of the cancellous bone.

**Keywords** Primary guinea pig osteoarthrosis · Alendronate · 3-D Microarchitecture · Mechanical properties · Bone collagen and mineral

M. Ding · I. Hvid
Orthopedic Research Laboratory, Department of Orthopedics, Aarhus University Hospital, Aarhus, Denmark

M. Ding (✉)
Orthopedic Research Laboratory, Department of Orthopedics, Odense University Hospital, Winsløwparken 15, 3.sal 8, DK-500 Odense C, Denmark
e-mail: ming.ding@ouh.regionsyddanmark.dk

C. C. Danielsen
Department of Connective Tissue Biology, Institute of Anatomy, University of Aarhus, Aarhus, Denmark

It is now generally recognized that osteoarthrosis (OA) is a complex multifactorial disease process involving the whole synovial joint including the articular cartilage, subchondral bones, synovium, and tendons. Three subchondral mineralized tissues, i.e., calcified cartilage, cancellous bone, and cortical bone, are different in the morphology, physiology, and mechanical properties and respond to mechanical and pharmacological stimuli in different ways through processes of growth, modeling, and remodeling [1]. It has long been a subject of debate whether subchondral bone changes in OA precede, concur with, or follow cartilage degeneration. Generally, there are two opposing hypotheses: bone sclerosis is secondary to cartilage loss and the result of cartilage breakdown and cartilage degeneration and loss are secondary to bone sclerosis—the Radin hypothesis. The Radin hypothesis emphasizes that thickening of subchondral bone increases internal cartilage stress, leading to increased hardening of the subchondral bone (sclerosis) and progressive thinning of articular cartilage [2, 3].

On ethical grounds, it is difficult to obtain tissue samples from human early-stage OA. Investigations on the earliest pathological changes have been focused on animal models. Recent studies have shown that subchondral plate and subchondral cancellous bone contribute significantly to OA initiation and progression as an increased subchondral bone density (volume fraction) results in the overloading and damage of the cartilage [4, 5]. Thickening of the subchondral plate in macaque monkeys precedes cartilage fibrillation, which might be due to increased resistance to compression of the bone [4]. The most fully described model of knee OA is the Dunkin-Hartley strain guinea pig, which shares the characteristics of human knee OA and is biochemically, histologically, and radiologically similar to human OA. Using this spontaneous OA animal model, we have currently demonstrated that the subchondral plate is involved in OA initiation and that subchondral cancellous bone is affected in both OA initiation and progression in a primary OA guinea pig model [6]. Furthermore, we have shown that hyaluronan treatment effectively protects against cartilage degeneration. Concomitantly, hyaluronan reduces subchondral bone density and thickness and delays the change in trabecular structure from rod-like to plate-like. Thereby, the subchondral bone becomes more compliant and expectedly may reduce cartilage stress during impact loading [7]. Thus, a more compliant subchondral bone may have beneficial effects on articular cartilage. This suggestion could be supported if a less compliant subchondral bone could be induced and demonstrated to augment the cartilage degeneration. At present, little is known about such a worsening, opposite effect of bone compliance, i.e., increased density and changed microarchitecture of subchondral bone on articular cartilage degeneration in the OA guinea pig model.

Bisphosphonates are potent agents that inhibit bone loss and increase bone mineralization and have been used clinically for the treatment of hypercalcemia of malignancy, osteoporosis, Paget's disease, and bone metastases. Bisphosphonates have been demonstrated to improve the three-dimensional (3-D) microarchitecture of cancellous bone [8], affect cancellous bone apparent modulus [9], and increase bone density and degree and uniformity of mineralization in cancellous bone [10]. However, high-dose bisphosphonates that inhibit bone remodeling will lead to microdamage accumulation in bone tissues [11, 12].

The aim of this study was to increase subchondral bone density and subsequently to examine the effect on cartilage degeneration in the OA guinea pig model. Specifically, we investigated the effects of increased bone density by inhibition of bone remodeling using alendronate (ALN) on the articular cartilage and 3-D microarchitecture and mechanical properties of bone tissues in a primary OA pig model, rather than assessing a direct or indirect effect of ALN on cartilage. Thus, we tested the hypothesis that increased bone density in subchondral bone tissues led to significant articular cartilage damage.

## Materials and Methods

### Experimental Animals

Sixty-six male Charles River strain outbred Dunkin-Hartley guinea pigs were purchased (HB Lidköpings Kaninfarm, Lidköping, Sweden) and used in this study. All the guinea pigs were acclimated for a period of 2 months before the experiment was started. The guinea pigs were housed in environmentally controlled cages, two or three in each cage. They were fed standard guinea pig chow containing 18% protein, 0.9% calcium, 0.7% phosphorus, and 600 IU/kg vitamin $D_3$ (Altromin Standard Guinea Pig Chow 3020; Altromin, Lage, Germany). Food and water were available at all times. The experimental protocol was in accordance with the Danish Animal Research guidelines and approved by the Danish Animal Experiment Committee (study J.nr. 2000/561–329).

### Experimental Design

Guinea pigs were randomly divided into six groups with similar ages and body weights (985–1,061 g). The treatments started in all groups when the guinea pigs were 6.5 months of age. Two groups received ALN 10 μg/kg, two groups received ALN 50 μg/kg, and two groups received vehicle (1 mL physiological saline) subcutaneously injection twice a week for 9 weeks. At 9 months of age, one 10 μg/kg group, one 50 μg/kg group, and one control group (9-week groups, $n = 3 \times 10$) were killed. The remaining three groups received once more the same treatment regimen (ALN 10 μg/kg, ALN 50 μg/kg, or saline injections for an additional 8 weeks). The latter three groups (17-week groups, $n = 3 \times 12$) were killed when the animals were 12 months old. Physical well-being and activity were checked daily, and body weights were measured weekly. At the completion of the experiment, the guinea pigs were killed and the left tibiae were dissected and kept in sealed plastic bags at −20°C. The right tibiae were used in another study.

### Micro-Computerized Tomography

The proximal tibiae were scanned using a high-resolution micro-computerized tomographic (micro-CT) system (μCT 40; Scanco Medical, Bassersdorf, Switzerland) to quantify

the microarchitecture of the subchondral bone plate. After this first scan, the proximal tibia was cut 0.5 mm beneath the subchondral plate and a further cut was made at the distal part to produce a 3-mm-thick cancellous–cortical complex bone specimen using a Leitz Microtome 1600 (Ernst Leitz, Wetzlar, Germany). Then, the second scan was made on this cortical–cancellous bone complex to quantify the microarchitecture of the subchondral cancellous bone and cortical bone. The scanned images had 3-D reconstruction cubic voxel sizes of 16 * 16 * 16 $\mu m^3$ (1,024 × 1,024 pixels) with 16-bit gray levels. The micro-CT images were segmented using the segmentation techniques described in detail previously [13] with slight modification [6] to obtain accurate 3-D imaging data sets for subchondral bone plate, cancellous bone, and cortical bone [6] (Fig. 1).

### 3-D Microarchitectural Properties of Subchondral Bone Plate

The subchondral plate was defined according to the previous description as beginning from the calcified cartilage–bone junction and ending at the marrow space [4, 7].

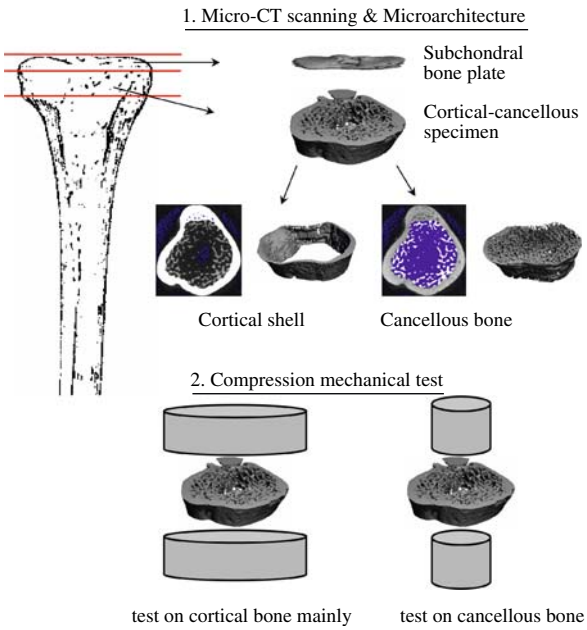


**Fig. 1** Study protocol. The proximal 4 mm of tibiae were scanned by micro-CT for quantification of 3-D microarchitecture of the subchondral bone plate. Then, a 3-mm-thick cancellous–cortical bone complex specimen was produced 0.5 mm beneath the subchondral plate. This complex specimen was scanned by micro-CT to quantify the microarchitecture of subchondral cancellous and cortical bones. The reduced platen test was first performed on cancellous bone only, then the compression test was done on the remaining cortical bone to determine their mechanical properties (see text) [6]

### 3-D Microarchitectural Properties of Subchondral Cancellous Bone

Subchondral cancellous bone was defined as the epiphyseal cancellous bone region 0.5 mm beneath the subchondral plate. The micro-CT imaging of the cancellous bone was segmented and separated from the cortical shell. The microarchitectural properties of the cancellous bone were calculated using true, unbiased, and assumption-free 3-D methods [7, 14, 15].

### 3-D Microarchitectural Properties of Subchondral Cortical Bone

Subchondral cortical bone was defined as the cortical bone shell in the region from 0.5 mm beneath the subchondral plate and 3 mm distally. The micro-CT imaging data of the cortical bone were segmented and separated from those of the cancellous bone [7]. The cortical thickness and cross-sectional area were the mean values obtained for the cortical shell.

### Grading Degree of OA

After micro-CT scanning, the sectioned articular cartilage and subchondral plate complexes from the proximal tibia were embedded in methylmethacrylate (MMA) and three slices (8 μm in thickness) from each medial condyle and lateral condyle were sectioned using a universal heavy-duty microtome (Reichert-Jung Cambridge Instruments, Nussloch, Germany). These cartilage slices were stained with safranin O staining. Then, the degree of cartilage degeneration was defined and graded according to the criteria of Mankin et al. [16]. This grading was based on assessment of the integrity of articular cartilage structure, loss of staining, and number of chondrocytes and was done blindly by two persons.

### Compression Testing of Proximal Tibiae

Mechanical tests of the proximal tibia 3-mm cancellous–cortical complex specimens were performed on an 858 Bionix MTS hydraulic material testing machine (MTS Systems, Minneapolis, MN), using a 1 kN load cell. The first compression test was performed after 10 preconditioning cycles compressing to 10% strain in the axial loading direction on the central cancellous bone only, thus keeping remaining peripheral trabeculae and cortex intact (reduced platen test) [17]. The second compression test was then performed on the cortical shell mainly [6]. Mechanical

properties were calculated from stress–strain curves derived from the recorded load-deformation curves [18]. The cross-sectional area used for normalization was, for trabecular bone, the contact area of the testing column and, for cortical bone, the mean cross-sectional area of the proximal and distal ends of the specimen (measured from micro-CT images) minus the contact areas of the testing columns for the reduced platen test (6) (Fig. 1).

### Determination of Bone Density, Collagen, and Mineral

After mechanical testing, the 3-mm-thick specimen was defatted. Thereafter, the dry weight and submerged weight (based on Archimedes' principle) of the specimens were measured (Mettler AT250 Delta Range balance; Mettler-Toledo, Greifensee, Switzerland) [18]. The determination of dry weight and submerged weight was repeated once. The total bone volumes of the specimens were determined from micro-CT images. Bone tissue density (g/cm$^3$) and apparent density (g/cm$^3$) of the specimens were calculated [18]. Then, the specimens were sectioned into medial and lateral condyle subspecimens. Two pieces from each condyle, after determination of the dry weight of the pieces, were used for collagen and mineral determinations according to a previously described procedure [18]. Thus, collagen content was estimated by measuring hydroxyproline, assuming a content of hydroxyproline in collagen of 13.4% (w/w). Hydroxyproline was determined by a colorimetric assay after hydrolysis of bone pieces. Mineral was estimated after incineration of the bone pieces in a muffle oven and determination of dry weight of the ash. Collagen and mineral contents were normalized with the dry weight of the bone pieces to derive collagen and mineral percentages and the collagen/mineral ratio.

### Statistical Analysis

The results (mean with standard deviation [SD]) were analyzed statistically using SPSS version 10.0.7 software (SPSS Inc., Chicago, IL). Normality and equal variance of the data were examined first. One-way analyses of variance (ANOVA) were performed among the three groups in each of the two experimental periods, and post-hoc multiple comparisons were adjusted using the Bonferroni test or Dunnett's test as appropriate. $P < 0.05$ was considered significant.

## Results

At death, the mean body weights (1,116–1,177 g) and the mean body weight gain (90–191 g) did not differ between the six groups.

Progressive cartilage degeneration was seen in both condyles of the guinea pigs (Fig. 2). Both 9- and 12-month-old guinea pigs developed typical osteopathy that was similar to human OA. Thus, chondrocyte death and proteoglycan loss with cartilage fibrillation were seen on the medial tibial plateau in all six groups. Incidence and severity of the cartilage lesions increased with age, and at 12 months of age the control animals had moderate degeneration in both the medial and lateral tibial condylar cartilage. Interestingly, the ALN-treated groups had more severe cartilage degeneration in the medial condyle and in the lateral condyle in the 9-week groups compared with controls (Fig. 2).

The 3-D reconstruction of proximal tibial subchondral bone tissues is demonstrated in Figure 3. Significant

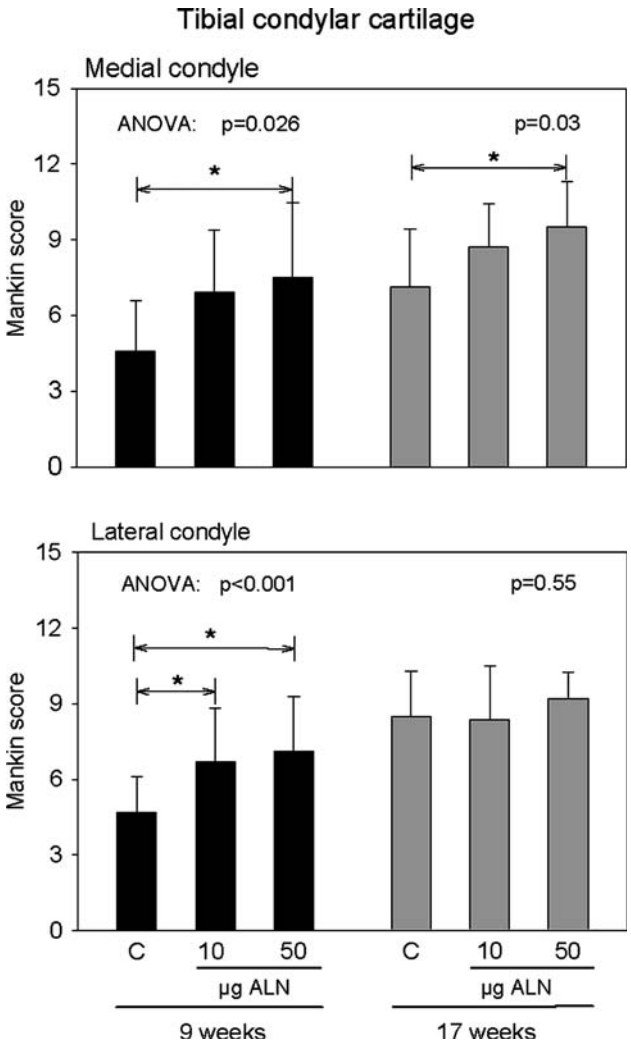


**Fig. 2** Mankin score for medial and lateral condylar cartilage. Subchondral bone plate thickness. Mean and SD (vertical bar). One-way ANOVA was performed among the three 9-week groups and the three17-week groups, and the resulting *P* values are indicated. *$P < 0.05$ when 10 µg and 50 µg ALN groups were compared with controls (C) of the same age (post-hoc multiple comparisons)

microarchitectural changes by inhibition of bone remodeling with ALN can be observed. In the 9-week groups, the 50 μg/kg ALN treatment resulted in significantly increased lateral subchondral bone plate thickness compared with controls (Fig. 4). In the control groups, an age-related increment in the plate thickness to a higher level was apparent in the 17-week group. However, ALN treatment did not increase the plate thickness above this higher level of the 17-week control group.

One of the most striking features after ALN treatment was microarchitectural changes in the subchondral cancellous bone (Table 1, Fig. 5). Thus, ALN treatment resulted in significantly increased cancellous bone volume fraction, connectivity density, and bone surface density. In addition, the trabeculae became more plate-like in structure (reduced structure model index) with reduced preferential orientation (architectural anisotropy) and separation. The changes in trabecular bone appeared after 9 weeks of treatment, with only a minor dose response of the doses given, and prolonged ALN treatment did not accentuate the difference between the ALN-treated groups and controls.

The most outstanding changes in the 3-D microarchitecture of subchondral cortical bone following ALN treatment were a greater cortical thickness and cross-sectional area, with an effect of ALN that appeared to increase with both ALN dose and treatment period (Fig. 6).

ALN treatment induced compositional changes in the subchondral bone (Table 2). Thus, following ALN treatment, the collagen concentration was reduced and the mineral concentration was increased. These changes were mirrored in a reduced collagen/mineral ratio and an increased tissue density. Also, the apparent density

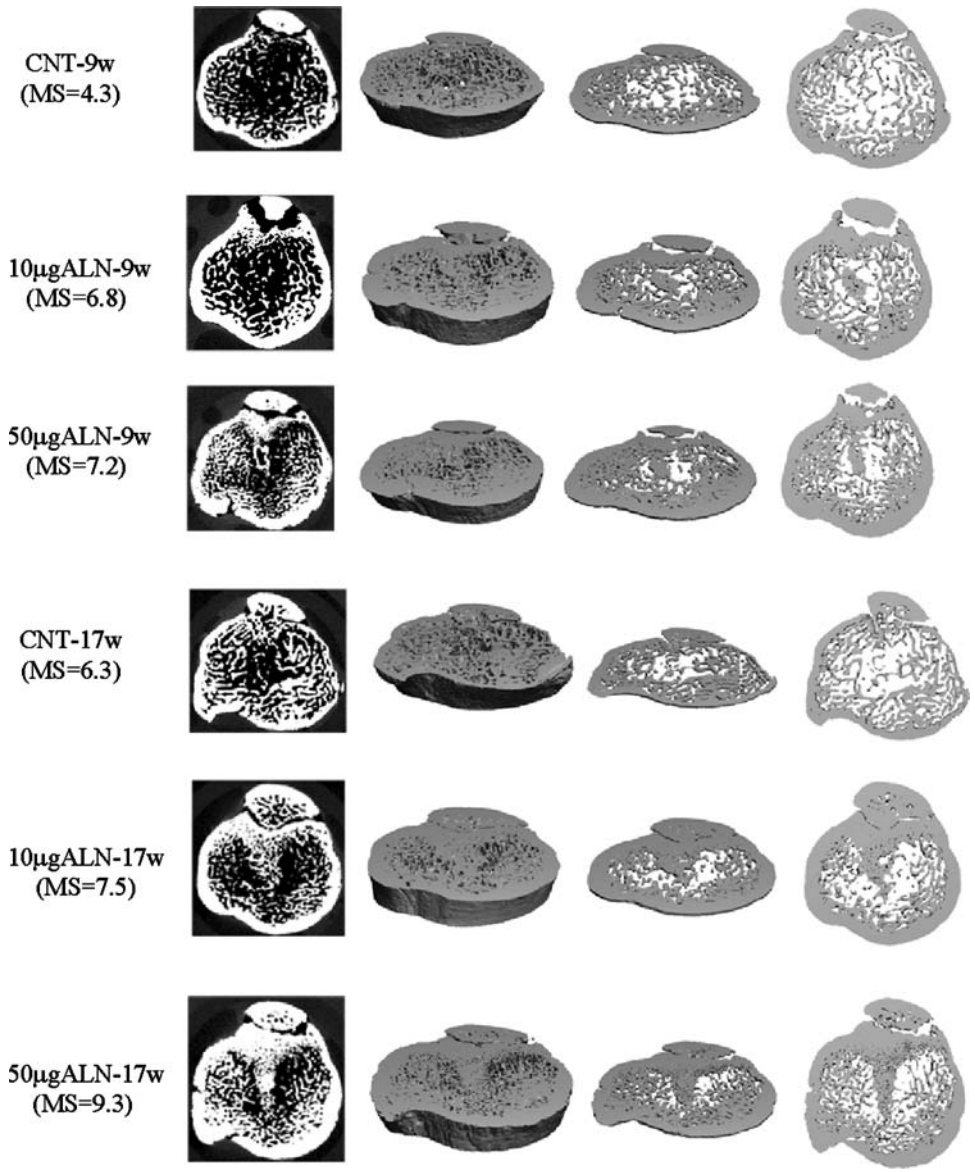


**Fig. 3** 3-D reconstruction of proximal tibial subchondral bone tissues from micro-CT imaging. Significant microarchitectural changes by inhibition of bone remodeling with ALN can be observed. These changes are supported by alteration of microarchitectural parameters; e.g., in all the ALN groups, bone density was increased, with more densely packed and extremely plate-like trabeculae and thicker cortex. MS, Mankin score

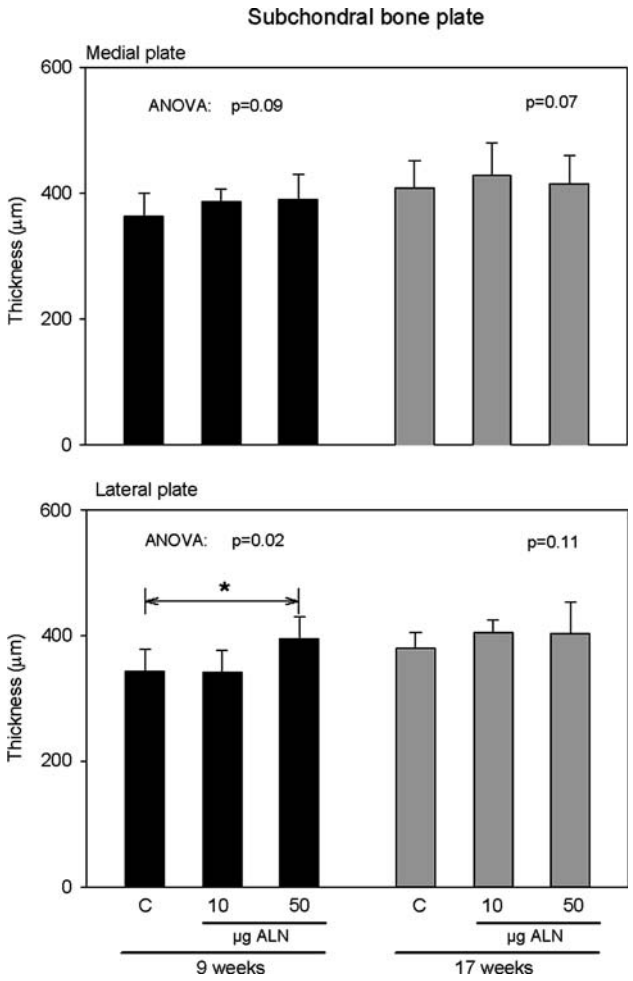


**Fig. 4** Thickness of medial and lateral subchondral plate. *$P < 0.05$ when 10 µg and 50 µg ALN groups were compared with controls (C) of the same age (post-hoc multiple comparisons)

increased. These changes appeared more pronounced after 17 weeks of treatment but were minimally influenced by ALN dose.

Treatment with ALN did not significantly influence the normalized mechanical properties of cancellous bone (Fig. 7). In cortical bone, high-dose ALN treatment increased ultimate stress in both the 9- and 17-week groups (Fig. 7). In addition, both doses of ALN either tended to (in the 9-week groups) or were found to (in the 17-week groups) increase failure energy. Low-dose ALN treatment increased ultimate strain in the 9-week and, more markedly, in the 17-week groups.

## Discussion

The present results on proximal tibia demonstrate ALN treatment–induced increments in subchondral cancellous and cortical bone volumes. In addition, pronounced microarchitectural changes of cancellous bone, increased densities and mineralization of subchondral bone, and elevated normalized ultimate stress of the subchondral cortical bone shell were found. All these changes to some extent were accompanied by increased articular cartilage degeneration (Mankin score). However, subchondral plate thickness was found to be significantly increased only in the lateral condyle in the 9-week group treated with 50 µg ALN/kg. Though the present results indicate accumulation of subchondral bone following ALN treatment, this accumulation is not followed by significant changes in elastic properties (Young's modulus) of the subchondral bone. Therefore, these data only partially support the hypothesis that increased subchondral bone density leads to significant articular cartilage damage.

In this study, ALN was given in two doses, 10 µg/kg and 50 µg/kg twice a week, which were estimated to represent similar and fivefold the clinical dose, respectively. These doses appear to have a dose-dependent antiresorptive effect on both cancellous and cortical bone as evident from the increases in cancellous bone volume fraction and in cortical thickness and cross-sectional area. We previously demonstrated that 6-month-old male guinea pigs had initiated OA, 9-month-old guinea pigs had typical OA, and 12-month-old guinea pigs had severe OA [6]. This study was initiated when the guinea pigs were 6.5 months old. Thus, when the guinea pigs were killed at 9 months or 12 months, typical OA or severe OA had developed in the control groups [6]. Dunkin-Hartley guinea pigs develop

**Table 1** 3-D microarchitectural properties of subchondral cancellous bone

| | 9-week experimental period | | | | 17-week experimental period | | | |
|---|---|---|---|---|---|---|---|---|
| | Control | 10 µg ALN | 50 µg ALN | ANOVA *P* | Control | 10 µg ALN | 50 µg ALN | ANOVA *P* |
| Trabecular thickness (µm) | 134 ± 12 | 128 ± 24 | 153 ± 42 | 0.14 | 145 ± 12 | 151 ± 47 | 140 ± 23 | 0.72 |
| Architecture anisotropy (–) | 1.83 ± 0.08 | 1.64 ± 0.09* | 1.64 ± 0.08* | <0.001 | 1.67 ± 0.13 | 1.64 ± 0.07 | 1.67 ± 0.06 | 0.58 |
| Bone surface density ($mm^{-1}$) | 5.78 ± 0.95 | 8.05 ± 1.20* | 7.39 ± 0.84* | <0.001 | 6.79 ± 0.35 | 8.02 ± 1.29* | 7.67 ± 0.53 | 0.007 |
| Trabecular separation (µm) | 367 ± 97 | 214 ± 65* | 204 ± 50* | <0.001 | 267 ± 27 | 192 ± 26* | 217 ± 34* | <0.001 |

Mean ± SD. The resulting *P* values obtained by one-way ANOVA are given

*$P < 0.05$ compared with control of the same age (post-hoc multiple comparisons)

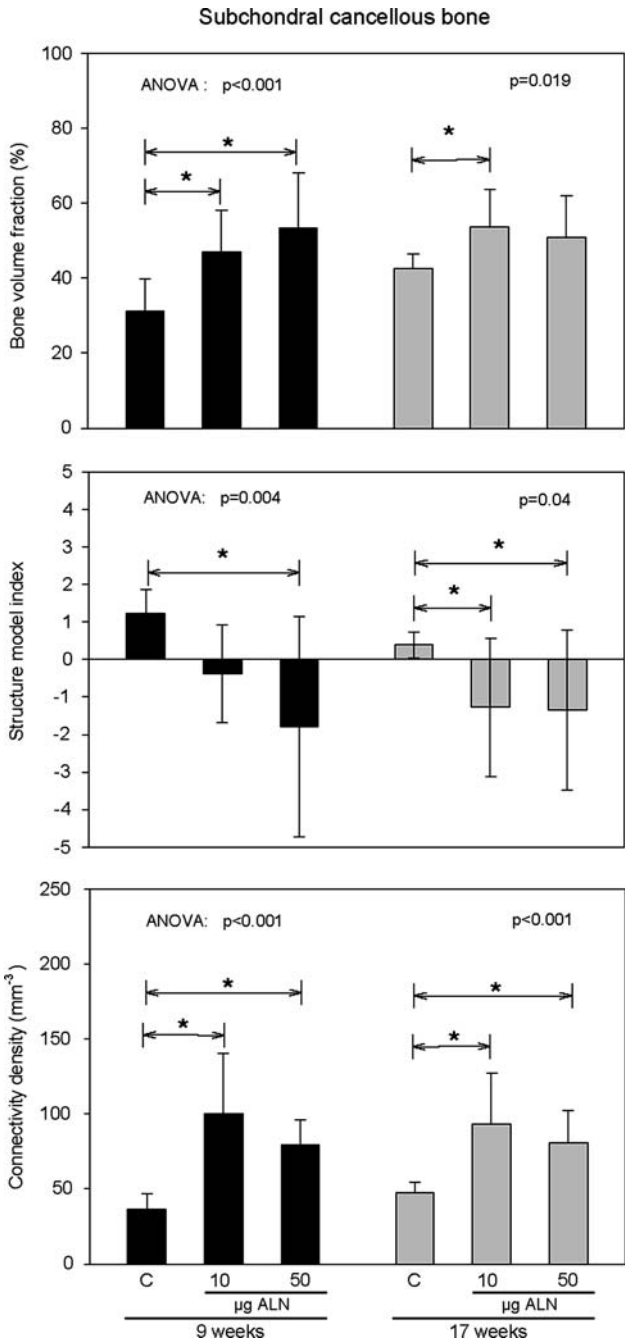


**Fig. 5** Subchondral cancellous bone volume fraction, structure model index, and connectivity density. *$P < 0.05$ when 10 µg and 50 µg ALN groups were compared with controls (C) of the same age (post-hoc multiple comparisons)

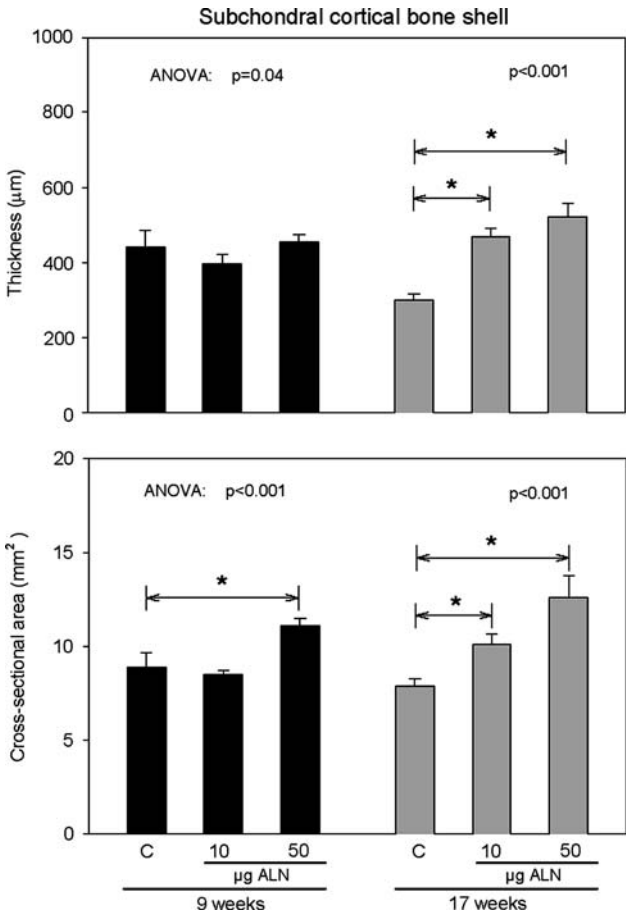


**Fig. 6** Thickness and cross-sectional area of the subchondral cortical bone shell. *$P < 0.05$ when 10 µg and 50 µg ALN groups were compared with controls (C) of the same age (post-hoc multiple comparisons)

primary OA at an early age, much earlier than that at which humans do [19, 20]. During the experimental period the guinea pigs gained weight. This weight gain occurred from 6.5 to 9 months of age since the weights of the six groups (9 and 12 months old) were very similar at death. This growth may accelerate OA progression [6]. However, ALN treatment accelerated OA progression to a great extent.

In a previous study on cynomolgus macaques, OA-increased subchondral plate thickness was directly associated with increased severity of cartilage lesions in the knee joint and animals with low subchondral plate thickness did not have cartilage lesions [4]. In the present study, the association between subchondral plate thickness (Fig. 4) and Mankin score (Fig. 1) appears not to be unequivocal. Thus, in the medial condyle, the subchondral plate thickness was not found to be different in any of the treatment periods, whereas the Mankin score increased with the ALN dose in both treatment periods. Truly, in the lateral condyle, both thickness and Mankin score either showed some coordinated increments (in the 9-week groups) or were not found to be different (in the 17-week groups) upon ALN treatment. Conflicting results for the association between subchondral plate thickness and Mankin score were also apparent in a previous study [7], where hyaluronan treatment for 2.5 and 5.5 months was associated with nearly absent cartilage degeneration after both treatment periods but with a reduced and an unchanged plate thickness,

**Table 2** Collagen and mineral composition and density of subchondral bone tissue

| | 9-week experimental period | | | | 17-week experimental period | | | |
|---|---|---|---|---|---|---|---|---|
| | Control | 10 μg ALN | 50 μg ALN | ANOVA *P* | Control | 10 μg ALN | 50 μg ALN | ANOVA *P* |
| Collagen concentration (%) | 17.2 ± 2.1 | 16.6 ± 2.3 | 17.4 ± 1.3 | 0.59 | 19.4 ± 1.8 | 16.8 ± 1.9* | 17.4 ± 1.4* | 0.004 |
| Mineral concentration (%) | 67.3 ± 2.7 | 69.8 ± 1.1* | 69.7 ± 2.1* | 0.01 | 66.9 ± 1.9 | 70.0 ± 1.6* | 71.2 ± 1.0* | <0.001 |
| Collagen/mineral ratio | 0.26 ± 0.03 | 0.24 ± 0.03 | 0.25 ± 0.02 | 0.25 | 0.29 ± 0.03 | 0.24 ± 0.03* | 0.25 ± 0.02* | <0.001 |
| Tissue density (g/cm$^3$) | 2.30 ± 0.08 | 2.32 ± 0.01 | 2.32 ± 0.02 | 0.35 | 2.16 ± 0.06 | 2.33 ± 0.02* | 2.35 ± 0.02* | <0.001 |
| Apparent density (g/cm$^3$) | 0.86 ± 0.10 | 0.98 ± 0.09 | 1.08 ± 0.14* | <0.001 | 0.94 ± 0.16 | 1.12 ± 0.13* | 1.12 ± 0.12* | 0.007 |

Mean ± SD. The resulting *P* values obtained by one-way ANOVA are given

*$P < 0.05$ compared with control of the same age (post-hoc multiple comparisons)

respectively, compared to controls [7]. Therefore, the association between subchondral plate thickness and cartilage degeneration does not seem straightforward in the OA guinea pig model [6, 7].

ALN treatment dramatically changed the microarchitecture of the subchondral cancellous bone in both the 9- and 17-week groups. Thus, ALN increased cancellous bone volume fraction, changed trabecular structure to extremely plate-like, decreased architectural anisotropy, and increased connectivity density (Table 1, Fig. 5). High-dose ALN treatment for 1 year was previously found to cause a significant increase in the mechanical properties of normal cancellous bone through microarchitectural adaptation [8], despite large accumulation of microdamage [12]. However, in this OA model, the changes in microarchitecture may have great significance. Thus, it has been well documented that bone strength depends on bone volume, microarchitecture, degree of mineralization, and bone remodeling [21]. The observed increased cancellous bone volume fraction, increased mineral concentration in the subchondral cortical–cancellous bone (Table 2), and change to plate-like trabeculae upon ALN treatment are all suggested to contribute to a higher mechanical stress [6]. However, the concomitant reduction in architectural anisotropy, i.e., reduction in axial trabecular orientation (which was significant in the 9-week groups), may be the reason for the insignificant increase in ultimate stress and Young's modulus of cancellous bone in the axial direction (Fig. 7). Also, the accumulation of microdamage in consequence of suppressed bone turnover by bisphosphonates [11, 12] may negatively influence mechanical strength. Taken together, the fact that the increased total amount of bone volume could not show parallel increased mechanical properties is likely due to deterioration of OA subchondral bone quality [5].

The present study showed that ALN treatment resulted in significantly greater thickness and cross-sectional area of the subchondral cortical shell, with the most marked changes after 17 weeks of treatment (Fig. 6). The accretion of cortical bone clearly indicates that bone formation prevails over bone resorption and thereby confirms the effect of ALN at the doses given. The increased cortical bone mass was accompanied by enhanced mechanical properties of the cortical bone (Fig. 7). This finding indicates that the cortical bone material added during the ALN treatment period has higher mechanical properties. The higher content of mineral, the increased tissue density, and the reduced collagen/mineral ratio in the subchondral cortical–cancellous specimen (Table 2) could be the explanation for this increment in mechanical properties. Thus, in cortical bone of normal female rats, an age-related decreasing collagen/mineral ratio and an increasing tissue density are coincidental with an increasing ultimate stress [22]. The importance of the cortical shell in OA progression is not known and has attracted little attention. However, the subchondral bone plate has a thickness similar to the cortical shell, and the thickness of the plate is influenced to some extent by ALN treatment. It could be speculated whether the mechanical properties of the cortical shell also are valid for the subchondral plate. Information about these properties, still to be obtained, in combination with those of the underlying cancellous bone could contribute to a better understanding of the total subchondral mechanical energy absorption capacity and the impact loading of the articular cartilage.

Besides an increased ultimate stress of the cortical shell following ALN treatment, the ultimate strain increased too (low-dose ALN). This change in ultimate strain could explain the absence of an increase in Young's modulus, which did not show significant changes. In addition, the mechanical properties of subchondral cancellous bone were not significantly changed. Therefore, any change in compliance of the subchondral bone and in the impact loading of the articular cartilage following ALN treatment is not unequivocally substantiated in the present study.

Recent studies have revealed that accelerated subchondral bone turnover is accompanied by specific structural changes in the cancellous bone of OA joints [23], abnormal bone mineral content [24, 25], and severalfold increased subchondral bone collagen metabolism in human femoral heads [25]. Whether subchondral changes exacerbate or

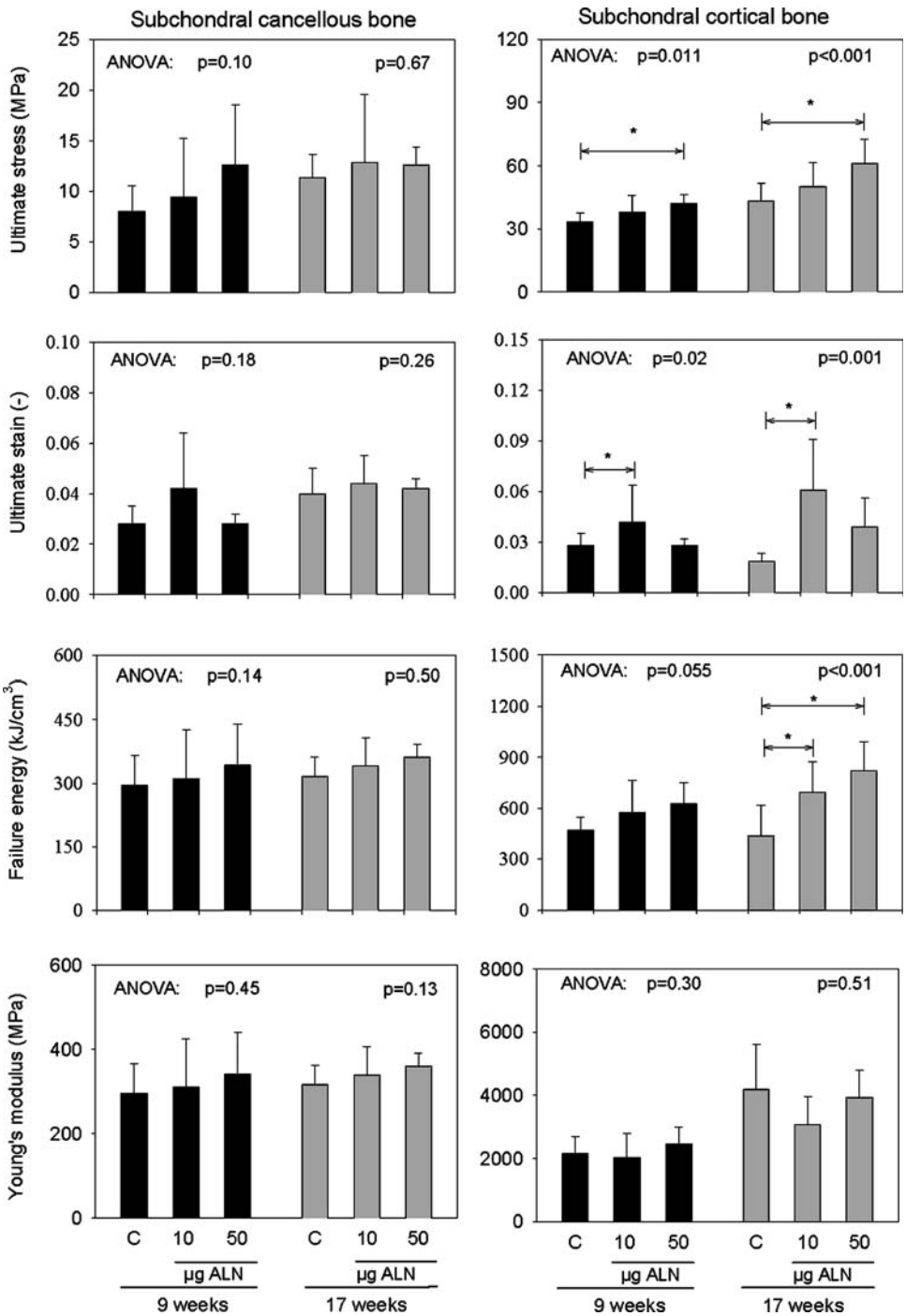


**Fig. 7** Ultimate stress of subchondral cancellous bone and subchondral cortical bone shell. $*P < 0.05$ when 10 µg and 50 µg ALN groups were compared with controls (C) of the same age (post-hoc multiple comparisons)

precede articular cartilage damage or vice versa in OA has been controversial and remains a subject of debate [26].

Hayami et al. [27] reported that ALN suppressed subchondral bone remodeling and was chondroprotective in a rat anterior cruciate ligament transection (ACLT) model of OA. However, the secondary OA, e.g., posttraumatic cartilage lesion, has a typical subchondral bone volume pattern with markedly decreased bone volume due to disuse right after the ACLT. However, in primary OA, the bone volume pattern is different with no temporary early drop in bone volume. Furthermore, the chondroprotective effect and the inhibitory effect on bone formation in the later phase of ALN as found by Hayami et al. [27] are not shown in the guinea pig model with primary OA in the present study.

It remains to be shown whether the subchondral bone changes and the articular cartilage degeneration in OA are mechanically coupled processes, metabolically coupled

processes, or coincidental processes mediated by growth factors/cytokines from other tissues (synovial membrane, capsule, ligaments, muscles, etc.) that are involved in the joint movements. To what extent ALN directly may affect chondrocytes or the cells in the other tissues is, at present, unknown. This issue was not investigated in the current study. We emphasize that the current investigation focused on the effects of ALN-inhibited remodeling of subchondral bone and we did not explore any potential effects of ALN on cartilage.

In conclusion, inhibition of bone remodeling by ALN significantly increased the subchondral bone mass, greatly changed the microarchitecture, and increased the bone mineral content and density. Furthermore, accelerated articular cartilage degeneration was observed at the medial condyle and, to some extent, at the lateral condyle. The mechanical properties increased significantly only for the subchondral cortical bone. Thus, the present results suggest that increased subchondral bone density promotes OA progression and call for circumspection in using bone density–enhancing drugs for intervention of primary OA.

**Acknowledgment** This study was supported by the Danish Rheumatism Association (Gigtforeningen, grant 233-949-11.07.00), Hørslev-fonden, and Helga og Peter Kornings Fond. We thank Jane Pauli, Anette Milton, and Eva K. Mikkelsen for skillful technical assistance and Ulla Dansberg and Hilmar Hald for animal care.

## References

1. Burr DB (2004) Anatomy and physiology of the mineralized tissues: role in the pathogenesis of osteoarthrosis. Osteoarthritis Cartilage 12(Suppl A):S20–S30
2. Radin EL, Paul IL, Rose RM (1972) Role of mechanical factors in pathogenesis of primary osteoarthritis. Lancet 1:519–522
3. Radin EL, Rose RM (1986) Role of subchondral bone in the initiation and progression of cartilage damage. Clin Orthop 213:34–40
4. Carlson CS, Loeser RF, Purser CB, Gardin JF, Jerome CP (1996) Osteoarthritis in cynomolgus macaques. III: Effects of age, gender, and subchondral bone thickness on the severity of disease. J Bone Miner Res 11:1209–1217
5. Ding M, Odgaard A, Hvid I (2003) Changes in the three-dimensional microstructure of human tibial cancellous bone in early osteoarthritis. J Bone Joint Surg Br 85:906–912
6. Ding M, Danielsen CC, Hvid I (2006) Age-related three-dimensional microarchitectural adaptations of subchondral bone tissues in guinea pig primary osteoarthrosis. Calcif Tissue Int 78:113–122
7. Ding M, Danielsen CC, Hvid I (2005) Effects of hyaluronan on three-dimensional microarchitecture of subchondral bone tissues in guinea pig primary osteoarthrosis. Bone 36:489–501
8. Ding M, Day JS, Burr DB, Mashiba T, Hirano T, Weinans H, Sumner DR, Hvid I (2003) Canine cancellous bone microarchitecture after one year of high-dose bisphosphonates. Calcif Tissue Int 72:737–744
9. Day JS, Ding M, Bednarz P, van der Linden JC, Mashiba T, Hirano T, Johnston CC, Burr DB, Hvid I, Sumner DR, Weinans H (2004) Bisphosphonate treatment affects trabecular bone apparent modulus through micro-architecture rather than matrix properties. J Orthop Res 22:465–471
10. Boivin GY, Chavassieux PM, Santora AC, Yates J, Meunier PJ (2000) Alendronate increases bone strength by increasing the mean degree of mineralization of bone tissue in osteoporotic women. Bone 27:687–694
11. Mashiba T, Hirano T, Turner CH, Forwood MR, Johnston CC, Burr DB (2000) Suppressed bone turnover by bisphosphonates increases microdamage accumulation and reduces some biomechanical properties in dog rib. J Bone Miner Res 15:613–620
12. Mashiba T, Turner CH, Hirano T, Forwood MR, Johnston CC, Burr DB (2001) Effects of suppressed bone turnover by bisphosphonates on microdamage accumulation and biomechanical properties in clinically relevant skeletal sites in beagles. Bone 28:524–531
13. Ding M, Odgaard A, Hvid I (1999) Accuracy of cancellous bone volume fraction measured by micro-CT scanning. J Biomech 32:323–326
14. Hildebrand T, Rüegsegger P (1997) Quantification of bone microarchitecture with the structure model index. Comput Methods Biomech Biomed Eng 1:15–23
15. Odgaard A (1997) Three-dimensional methods for quantification of cancellous bone architecture. Bone 20:315–328
16. Mankin HJ, Dorfman H, Lippiello L, Zarins A (1971) Biochemical and metabolic abnormalities in articular cartilage from osteo-arthritic human hips. II. Correlation of morphology with biochemical and metabolic data. J Bone Joint Surg Am 53:523–537
17. Hogan HA, Ruhmann SP, Sampson HW (2000) The mechanical properties of cancellous bone in the proximal tibia of ovariectomized rats. J Bone Miner Res 15:284–292
18. Ding M, Dalstra M, Danielsen CC, Kabel J, Hvid I, Linde F (1997) Age variations in the properties of human tibial trabecular bone. J Bone Joint Surg Br 79:995–1002
19. Bendele AM, Hulman JF (1988) Spontaneous cartilage degeneration in guinea pigs. Arthritis Rheum 31:561–565
20. Bendele AM, White SL, Hulman JF (1989) Osteoarthrosis in guinea pigs: histopathologic and scanning electron microscopic features. Lab Anim Sci 39:115–121
21. Friedman AW (2006) Important determinants of bone strength: beyond bone mineral density. J Clin Rheumatol 12:70–77
22. Danielsen CC, Mosekilde L, Svenstrup B (1993) Cortical bone mass, composition, and mechanical properties in female rats in relation to age, long-term ovariectomy, and estrogen substitution. Calcif Tissue Int 52:26–33
23. Burr DB (1998) The importance of subchondral bone in osteoarthrosis. Curr Opin Rheumatol 10:256–262
24. Grynpas MD, Alpert B, Katz I, Lieberman I, Pritzker KP (1991) Subchondral bone in osteoarthritis. Calcif Tissue Int 49:20–26
25. Mansell JP, Bailey AJ (1998) Abnormal cancellous bone collagen metabolism in osteoarthritis. J Clin Invest 101:1596–1603
26. Bailey AJ, Mansell JP (1997) Do subchondral bone changes exacerbate or precede articular cartilage destruction in osteoarthritis of the elderly? Gerontology 43:296–304
27. Hayami T, Pickarski M, Wesolowski GA, McLane J, Bone A, Destefano J, Rodan GA, Duong T (2004) The role of subchondral bone remodeling in osteoarthritis: reduction of cartilage degeneration and prevention of osteophyte formation by alendronate in the rat anterior cruciate ligament transection model. Arthritis Rheum 50:1193–1206